In this study, we also incorporated the pore water pressure (R_u) coefficient to simulate different water saturation conditions by assuming constant moisture levels at different depths. The obtained FoS values were 0.75, 0.71 and 0.69 for dry static, pseudo-static and wet conditions respectively (Figure 6 *c*) and thereby supporting a precarious slope.

This study describes the causative factors and failure mechanism responsible for triggering the Birik Dara landslide and also analyses the stability of the slope using diverse methods. A side-by-side comparison of the applied rock mass classification techniques, including kinematic analysis, reveals that the slope section is critically unstable, which has been further strengthened by FEM analysis (FoS ≤ 1). Although this landslide does not pose any direct risk to the settlements, it has a strong propensity to damage NH-10 and may affect the traffic. After the 2021 incident, the road was cleared for transportation, but it may be damaged again due to future rainfall/earthquake events. Considering the strategic significance of NH-10 as the only route for the people of Sikkim and Kalimpong to connect with the rest of India, it is imperative to develop appropriate stability measures to avoid future disastrous situations. The rationale behind this study is to ensure safe operation in this area, and also provide guidance to the decision-makers for landslide hazard mitigation and environmental remediation.

1. Cruden, D. and Varnes, D., Landslide types and processes. In *Landslides: Investigation and Mitigation. Special Report 247*, National Research Council. Transportation Research Board, Washington, DC, USA, 1996.
2. Acharyya, S. K., Structural framework and tectonic evolution of the eastern Himalaya. *Himalayan Geol*., 1980, **10**, 412–439.
3. Goel, R. K. and Subhash, M., Importance of weathering in rock engineering. In International Conference on Engineering Geology in New Millennium, Indian Institute of Technology Delhi, New Delhi, 2015, pp. 231–245.
4. Hoek, E. and Bray, J. D., *Rock Slope Engineering*, CRC Press, 1981, pp. 36–38.
5. Bieniawski, Z. T., The geomechanics classification in rock engineering applications. In 4th ISRM Congress, Onepetro, 1979.
6. Palmstrom, A., Measurements of and correlations between block size and rock quality designation (RQD). *Tunnel. Underg. Space Technol*., 2005, **20**(4), 362–377.
7. Romana, M., New adjustment ratings for application of Bieniawski classification to slopes. In Proceedings of the International Symposium on Role of Rock Mechanics, Zacatecas, Mexico, 1985, pp. 49–53.
8. Sarkar, S., Pandit, K., Sharma, M. and Pippal, A., Risk assessment and stability analysis of a recent landslide at Vishnuprayag on the Rishikesh–Badrinath highway, Uttarakhand, India. *Curr. Sci*., 2018, **114**(7), 1527–1533.
9. Hoek, E. and Brown, E. T., Practical estimates of rock mass strength. *Int. J. Rock. Mech. Min*., 1997, **34**(8), 1165–1186.
10. Sonmez, H. and Ulusay, R., A discussion on the Hoek–Brown failure criterion and suggested modifications to the criterion verified by slope stability case studies. *Yerbilimleri*, 2002, **26**, 77–99.
11. Das, S., Sarkar, S. and Kanungo, D. P., GIS-based landslide susceptibility zonation mapping using the analytic hierarchy process (AHP) method in parts of Kalimpong Region of Darjeeling Himalaya. *Environ. Monit. Assess*., 2022, **194**(3), 1–28.

ACKNOWLEDGEMENTS. S.D. thanks Sushanta Biswas for his support during field survey and the TLD-IV PS administrators for providing rainfall data. We thank the Director, CSIR-Central Building Research Institute, Roorkee for permission to publish this work. S.D. also thanks the University Grants Commission, New Delhi for the Junior Research Fellowship (JRF) (UGC-Ref. No. 3511/(NET-JULY 2018)) and the Academy of Scientific and Innovative Research, Ghaziabad for providing an opportunity to carry out this doctoral research.

Received 20 December 2021; revised accepted 27 July 2022

doi: 10.18520/cs/v123/i7/928-933

Preliminary observations on computerized tomography-powered fractal dimension-based technique to differentiate between coprolites and body fossils

Shubhabrata Sarkar[1], Sanjukta Chakravorti[2,3,*], Sudhir Kumar Chaudhary[1], Dhurjati P. Sengupta[2], Pankaj Wahi[1] and Prabhat Munshi[1]

[1]Nuclear Engineering and Technology Programme, Indian Institute of Technology Kanpur, Kanpur 208 016, India
[2]Geological Studies Unit, Indian Statistical Institute, 203, Barrackpore Trunk Road, Kolkata 700 108, India
[3]Department of Earth Sciences and Remote Sensing, JIS University, 81 Nilgunj Road, Kolkata 700 109, India

This study presents a fossil signature based on fractal dimension (FD) derived from computerized tomography (CT) images to differentiate between coprolites and body fossils. Coprolites are generally studied using destructive techniques like thin section study and geochemistry. Coprolites and body fossils collected from the Triassic terrestrial Gondwana deposits of India were chosen for the study. The presented CT-powered FD-based digital signature can properly distinguish coprolites from other fossils, without losing the structural features of the samples. The present study will further enhance the digitalized fossil research.

Keywords: Computerized tomography, coprolites, fossils, fractal dimension, X-ray.

LITHIFIED fossil faeces (coprolites) are highly variable trace fossils (records of behaviour of organisms preserved in rocks). They pose an analytical challenge for palaeontologists owing to their variable texture and shape. The study of coprolites is important as they reflect upon the dietary

*For correspondence. (e-mail: chirpymoni2009@gmail.com)

residues of extinct animals. This in turn sheds light on trophic relationships, dietary efficiency, palaeo-ecosystems and thereby palaeoenvironment that were prevalent at the time the coprolites were produced[1]. The present study focuses on computerized tomography (CT), comparing fragmentary encrusted body fossils with encrusted coprolites using non-destructive techniques.

CT-based non-destructive testing is a popular and routine inspection method for a variety of objects, including fossil samples[2–8]. Earlier, micro-CT scanning was successfully applied as a non-destructive technique to study body fossils, their microanatomical data and skeleto-chronology[2]. It has been suggested as a good alternative to thin sectioning[2]. Recently, several non-destructive methods, like neutron tomography and structured light optical scanning, have also been successfully used for the morphological and compositional study of fossils[3]. Due to the rarity of fossils, the usage of CT is gradually gaining ground in palaeontological studies.

Here, we present and experimentally validate the use of fractal dimension (FD) as a digital signature to distinguish between coprolites and body fossils, both collected from the Triassic terrestrial Gondwana deposits of India. The general lithology of the terrestrial Gondwana deposits in India consists of red mudstone, calcareous sandstone and calcirudites. It is to be noted that the karstic environment within the terrestrial Gondwana deposits favours the permineralization of phosphates, thus making it difficult to distinguish between coprolites and fragmentary body fossils. The coprolites that are enriched with phosphate were once of potential use in the fertilizer industry from an economic point of view[4,5]. The technique using FD gives a distinct signature to distinguish between fragmentary body fossils and coprolites, as is evident from the present study. This can be extrapolated further for mineralogical studies to define the taphonomic process leading to the fossilization of a faecal matter, thus serving as an excellent method for reconstructing trophic structures and energy-flow models of past ecosystems[6].

Coprolites and body fossils collected from the Triassic (252–201 million years ago) terrestrial Gondwana deposits of India were chosen for the study. The experimental data have been obtained using the Procon X-ray CT mini machine installed at '*Divyadrishti Prayogshala*', IIT Kanpur with the following experimental specifications: X-ray tube voltage of 121 kV, X-ray tube current of 120 μA, exposure time of 400 mS and number of projections = 400. Figure 1 shows photographs and CT images of the examined body fossils and coprolites. Three coprolites were selected, of which ISI/COP/III had the maximum number of layers and inclusions. Thus it was sectioned and polished (Figure 1, III*d*). The polished section of the coprolite was prepared at Geological Studies Unit of the Indian Statistical Institute, Kolkata. The sections from the magnified study under the microscope were compared with the micro-CT images. Three well-identified body fossil fragments, along with coprolites, were chosen as a training dataset for comparison (Figure 1 IV*a*, IV*b*, V*a*, V*b*, Vi*a* and VI*b*). The body fossils comprised a fragmentary temnospondyl skull (ISI A 206) and temnospondyl post-cranial bones (Ilium ISI A 30 and vertebra ISI A 32) (Figure 1, IV*a*, IV*b*, V*a*, V*b*, VI*a* and VI*b*). The images were reconstructed using FDK (Feldkamp–Davis–Kress) algorithm and Volume Player Plus software was used for visualization. Table 1 lists the fossils and coprolites used with their corresponding horizons and specimen numbers.

Figure 2 shows photographs of the in-house CT scanner.

Fractals can be defined as intricate patterns which show self-similarity across several scales[7]. They represent a set whose Hausdorff–Besicovitch dimension strictly surpasses the topological dimension. If m is an integer and represents the smallest integer dimensional space among all feasible integer dimensional spaces that may encompass X and $N(\varepsilon)$, represents the number of m-dimensional spheres of diameter ε required to enclose X, then

$$N(\varepsilon) \propto \left(\frac{1}{\varepsilon}\right)^{D}, \tag{1}$$

where D is FD.

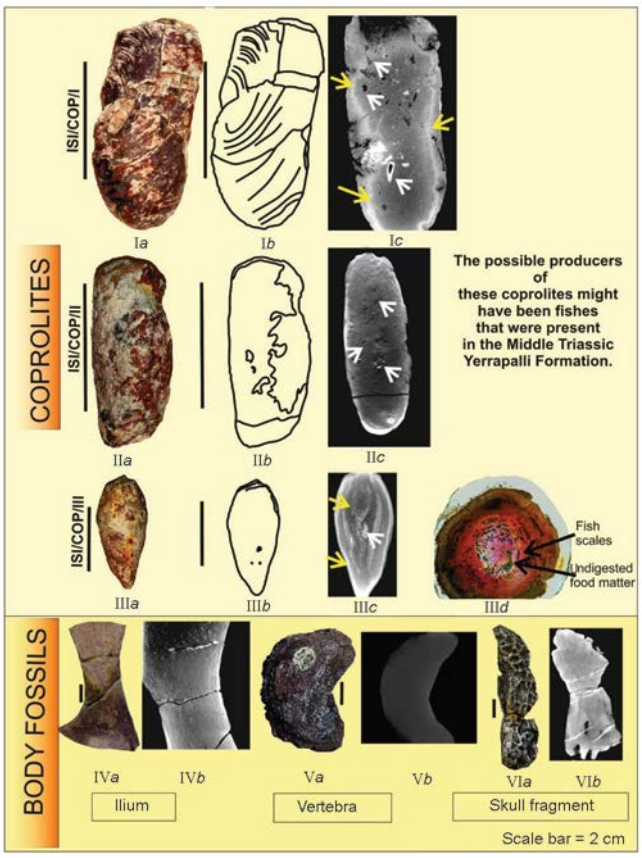

Figure 1. Different coprolites used in this study and their possible producers along with the body fossils used for comparison. Scale bar = 2 cm for the images; scale of the computerized tomography (CT) image is 1000 × 1000.

Table 1. Details of coprolites and body fossils used in this study

Specimen number	Identification of specimen	Locality and age
ISI/COP/I	Coprolite	Middle Triassic Yerrapalli Formation
ISI/COP/II	Coprolite	Middle Triassic Yerrapalli Formation
ISI/COP/III	Coprolite	Middle Triassic Yerrapalli Formation
ISI A 30	Chigutisaurid ilium	Late Triassic Maleri Formation
ISI A 32	Chigutisaurid vertebra	Late Triassic Maleri Formation
ISI A 206	Skull fragment of temnospondyl amphibian	Late Triassic Maleri Formation

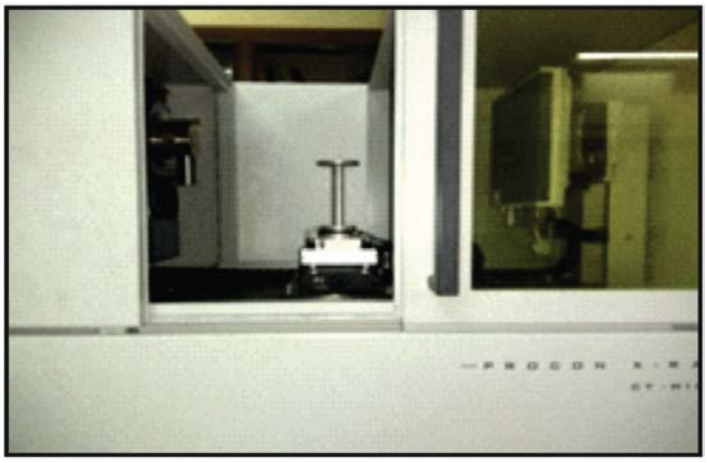

Figure 2. In-house Procon X-ray CT mini scanner.

Fractional Brownian motion (fBm) is one of the most effective fractal models to explain the geometrical complexity of objects. The fBm surface $I(x, y)$ is given by[8]

$$E(|I(x_2, y_2) - I(x_1, y_1)|) \propto \sqrt{(x_2 - x_1)^2 - (y_2 - y_1)^2}^{H}, \quad (2)$$

where $0 < H < 1$, and H is the Hurst coefficient. $E(|I(x_2, y_2) - I(x_1, y_1)|)$ denotes the mean value of the absolute difference $I(x_2, y_2) - I(x_1, y_1)$. D of the fBm surface is represented as

$$D = 3 - H. \quad (3)$$

A 2D image can be manifested in 3D using image intensity as the third dimension. As a result, a 2D image can be understood as a 3D structure with FD ranging from 2 to 3.

FD is an invaluable measure for understanding the complexity of shapes and organismal morphology[9]. Thus, it can be used as an appropriate index of quality for the CT images. Details regarding the calculation of FD by the Hurst coefficient are available in the literature[10,11]. In brief, let $I(u, v)$ represent the intensity of any pixel of an $M \times M$ pixel block image, where $u, v = 0, 1, 2 \ldots M - 1$. The FD graph of an image is the plot of log (NMSID) versus log (NSR), where NMSID is the normalized multi-scale intensity difference vector and NSR is the normalized scale range vector. A perfect fractal is indicated by a linear FD curve. A least squares linear regression on it yields the slope (H) of the resulting curve, from which FD is computed using the relationship $D = 3 - H$.

Real surfaces and images are unlikely to show fractal nature over all ranges of scale. Hence, it is a general practice to account for the values of NSR that exhibit linearity of the graph for estimation of FD.

Multiple methods were previously used to study coprolites biochemical morphological and thin-section studies[12–14]. However, non-destructive techniques remain far less studied and no work has been done to distinguish coprolites from fragmented body fossils. The studied specimens of coprolites had diagnostic features like the presence of inclusions (non-digested matter) (Figure 1, I*a*–I*c*, II*a*–II*c* and III*a*–III*d*), copro-fabrics, furrows reflecting a contraction of the sphincter (indicated by yellow arrows (Figure 1, I*c* and III*c*). These features distinguish the studied specimens from concretions. The cylindrical/coiled shape of the observed nodules is not consistent with the shape of chemical concretions or fluvial transported intraclasts, which further supports the studied specimens to be coprolites and not concretions. All the three coprolites chosen for the present study were found intact without any segmentation or breakage. ISI/COP/I (Figure 1, I*a*–I*c*) is amphipolar in nature. It is elongated and cylindrical in shape with a tapered and jagged anterior end and well-rounded posterior end. It has a brownish colour and bears an irregular texture due to exfoliation. Micro CT images reveal the presence of two

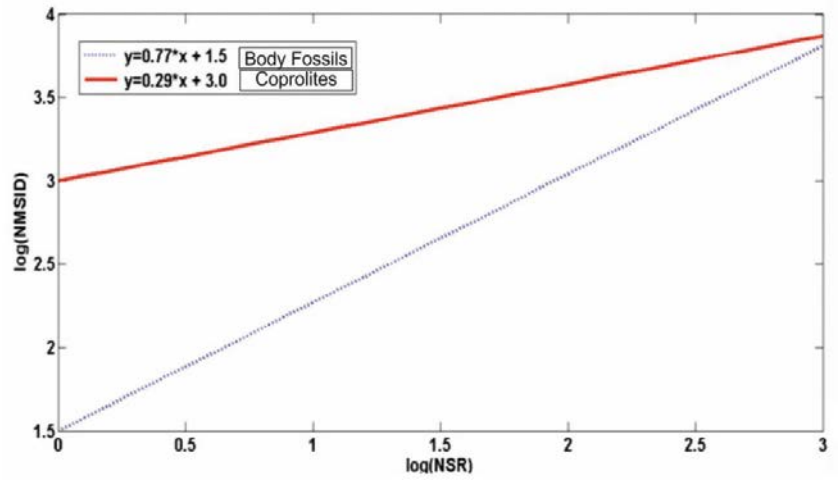

Figure 3. Superimposed best fit fractal dimension (FD) curves for the coprolites samples (red line) and body fossils (blue dotted line).

Table 2. Fractal dimension (FD) values for different coprolites and body fossils

Coprolite	FD value	Body fossil	FD value
ISI/COP/I	2.7000	Ilium of temnospondyl amphibian (ISI A 30)	2.3900
ISI/COP/II	2.6800	Vertebra of temnospondyl (ISI A 32)	2.2300
ISI/COP/III	2.7100	Skull fragment of temnospondyl amphibian (ISI A 206)	2.4900

whorls, the central whorl within the coprolite being slightly sphincteric in the middle. The presence of several inclusions of varied shapes like irregular, linear and circular can be noted (indicated by white arrows in Figure 1).

ISI/COP/II (Figure 1, II*a*–II*c*) is cylindrical, rod-shaped coprolite with rounded isopolar ends. The anterior end is rounded, while the posterior end is tapering and slightly narrower. Micro-CT image reveals only a single whorl within the coprolite and the presence of a few small circular inclusions. It has a rough texture and the colour is white with brown patches. ISI/COP/III (Figure 1, III*a*–III*d*) is ovoid and has an externally smooth texture. It has the highest number of parallel laminae/whorls (mucosal layers) among the three specimens chosen, as revealed in the micro-CT images. A total of five concentric whorls or laminae are presenting, along with a significant number of inclusions and undigested matter. Thus, this specimen was sectioned and a polished section was studied under reflected light to correlate with the micro-CT image. The polished section also revealed concentric whorls within the coprolite, along with several inclusions, undigested food matter and fish scales, as identified by reflected light microscopy (Figure 1, III*d*). Depending on their size, shape, presence of laminae and presence/absence/rarity of inclusions, three coprolites may belong to different species of fauna present in the Middle Triassic Yerrapalli Formation. This is because coprolites produced by various species of a taxon usually possess a different outline and morphology depending on the internal gut structure of the animals. This makes them an ideal training dataset based on the FD measure and for comparison with body fossils. Potential producers of coprolites might have been Osteichthyes (bony fishes) found in the Middle Triassic Yerrapalli Formation[15]. Fish scats generally exhibit spiral morphology at one end (hetero-polar) or spiral extending to both ends (amphipolar)[16,17]. These are produced by the spiral intestinal valve within the bony fishes. Bony fish faeces are usually amphipolarly spiral[6,15,18–20] and shark faeces usually show heteropolar spiral nature. Sohn and Chatterjee[21] suggested that the Triassic coprolites of the Indian Gondwana deposits were produced by large vertebrates.

Figure 3 shows the linear range FD curve for coprolite sample ISI/COP/I and the fossilized bone sample 'skull fragment'.

Table 2 shows the FD values for various fossil samples. Figure 4 shows FD curves for six specimens. The FD values are almost similar for coprolites and fossilized bones. However, the coprolites average (~2.70) is distinctly different from the corresponding average (~2.35) for the body fossils.

Although only a few specimens could be examined, the FD-based fossil signature derived from the CT images differentiates between coprolites and body fossils without affecting the structural integrity of the fossils. The material characterization performance of FD is dependent upon the resolution of the CT images, as the FD value depends on the resolution of the CT images[22]. In the present study, the data size is small, so it may be unwise to draw any strong conclusion from the results. The future research plan includes the study of the FD-based characterization technique with a

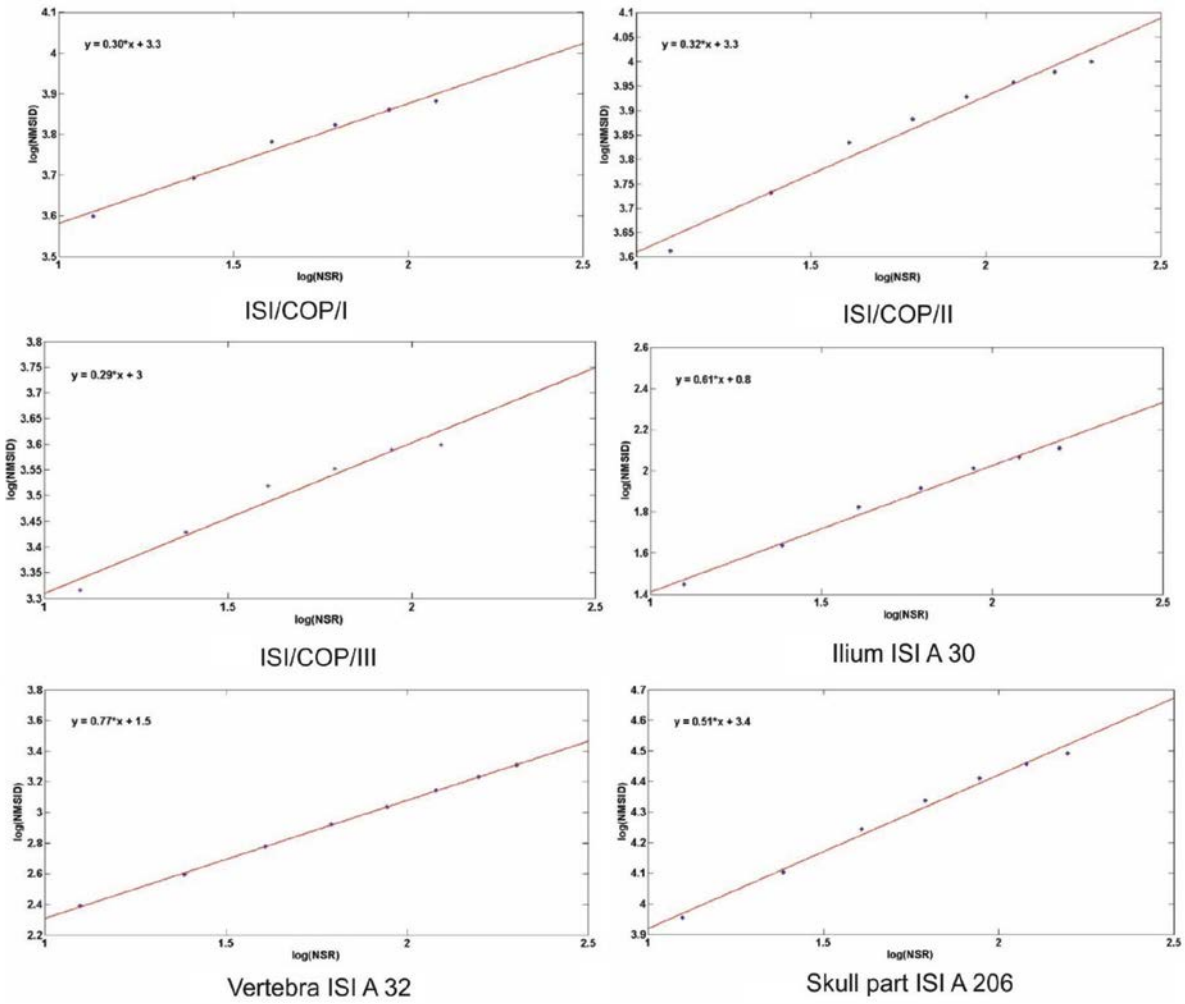

Figure 4. FD curves for six specimens.

larger set of fossil samples and varying the resolution of CT images for each sample. Nevertheless, preliminary observations depict that FD can be used as a powerful morphological digital signature for distinguishing coprolites from body fossils. The FD-based fossil signature can efficiently contribute to locating phosphate sources[5,6], as coprolites are enriched with phosphate. This will shed considerable light on the paleoenvironment prevalent in deep time and will strengthen the database to complete a trophic pyramid in India's Triassic terrestrial Gondwana deposits with details of prey–predator relationships.

Data accessibility: Raw CT scan files are available on request from the authors.

Conflict of interest: The authors declare that there is no conflict of interest.

1. Chin, K., Thin section analysis of lithified coprolites (fossil feces). *Microsc. Microanal.*, 2007, **13**, 50.
2. Konietzko-Meier, D. and Schmitt, A., A histological study of a femur of plagiosuchus, a Middle Triassic temnospondyl amphibian from southern Germany, using thin sections and micro-CT scanning. *Neth. J. Geosci.*, 2013, **92**, 97–108.
3. Maróti, B., Polonkai, B., Szilágyi, V., Kis, Z., Kasztovszky, Z., Szentmiklósi, L. and Székely, B., Joint application of structured-light optical scanning, neutron tomography and position-sensitive prompt gamma activation analysis for the non-destructive structural and compositional characterization of fossil echinoids. *NDT & E Int.*, 2020, **115**, 102295.
4. Ford, T. D. and O'Connor, B., Coprolite mining in England. *Geol. Today*, 2002, **18**, 178–181.
5. Grove, R., Coprolite mining in Cambridgeshire. *Agric. Hist. Rev.*, 1976, **24**, 36–43.
6. Luo, M. *et al.*, Taphonomy and palaeobiology of Early Middle Triassic coprolites from the Luoping biota, southwest China: implications for reconstruction of fossil food webs. *Palaeogeogr., Palaeoclimatol., Palaeoecol.*, 2017, **474**, 232–246.
7. Degiorgio, V., Mandelbrot, BB the fractal geometry of nature. *Rivista di Scienza*, 1984, **78**(119).
8. Chen, C.-C., DaPonte, J. S. and Fox, M. D., Fractal feature analysis and classification in medical imaging. *IEEE Trans. Med. Imag.*, 1989, **8**, 133–142.
9. Uppal, S. O. *et al.*, Pattern analysis of microtubule-polymerizing and -depolymerizing agent combinations as cancer chemotherapies. *Int. J. Oncol.*, 2007, **31**, 1281–1291.

10. Athe, P., Shakya, S., Munshi, P., Luke, A. and Mewes, D., Characterization of multiphase flow in bubble columns using KT-1 signature and fractal dimension. *Flow Meas. Instrum.*, 2013, **33**, 122–137.
11. Sarkar, S., Pandey, D., Rathore, K. and Munshi, P., Estimation of moisture content in edible pulses by the application of computerized tomography. NDE2015, Hyderabad, 2015, pp. 26–28.
12. Romaniuk, A. A. *et al.*, Combined visual and biochemical analyses confirm depositor and diet for neolithic coprolites from Skara Brae. *Archaeol. Anthropol. Sci*., 2020, **12**, 1–15.
13. Hunt, A. P. and Lucas, S. G., Crocodylian coprolites and the identification of the producers of coprolites. In *Crocodyle Tracks and Traces* (eds Milàn, J. *et al.*), New Mexico Museum of Natural History and Science, Bulletin 51, 2010, pp. 219–226.
14. Rakshit, N. and Ray, S., Bone-bearing coprolites from the Upper Triassic of India: ichnotaxonomy, probable producers and predator–prey relationships. *Pap. Palaeontol.*, 2022, **8**, e1418.
15. Jain, S. L., Spirally coiled coprolites from the Upper Triassic Maleri formation, India. *Palaeontology*, 1983, **26**, 813–829.
16. Schmitz, M. and Binda, P. L., Coprolites from the Maastrichtian Whitemud Formation of southern Saskatchewan: morphological classification and interpretation on diagenesis. *Paläontol. Z.*, 1991, **65**, 199.
17. Eriksson, M. E., Lindgren, J., Chin, K. and Månsby, U., Coprolite morphotypes from the Upper Cretaceous of Sweden: novel views on an ancient ecosystem and implications for coprolite taphonomy. *Lethaia*, 2011, **44**, 455–468.
18. McAllister, J. A., Reevaluation of the formation of spiral coprolites, The University of Kansas Paleontological Contributions-Paper 114, 1985.
19. Felker, C. D. H., Middle Eocene shark coprolites from shallow marine and deltaic coasts of the pre-North Sea Basin in Central Europe. *Vertebr. Coprolites: New Mexico Mus. Nat. Hist. Sci., Bull*., 2012, **57**, 311–318.
20. Dentzien-Dias, P. C., Poinar Jr, G., de Figueiredo, A. E., Pacheco, A. C., Horn, B. L. and Schultz, C. L., Tapeworm eggs in a 270 million-year-old shark coprolite. *PLoS ONE*, 2013, **8**, e55007.
21. Sohn, I. and Chatterjee, S., Freshwater ostracodes from Late Triassic coprolite in Central India. *J. Paleontol*., 1979, 578–586.
22. Toghyani, S., Nasseh, I., Aoun, G. and Noujeim, M., Effect of image resolution and compression on fractal analysis of the periapical bone. *Acta Inf. Med*., 2019, **27**(3), 167.

ACKNOWLEDGEMENTS. S.S. thanks Suman Roy (Department of Civil Engineering, IIT Kanpur) and Manab Mukherjee (Department of Earth Science, IIT Kanpur) for valuable suggestions and Dr Kavita Rathore (NETP, IIT Kanpur) for helping with the Matlab code for fractal dimension. S.C. and D.P.S. thank the Indian Statistical Institute, Kolkata for funds. We thank the two anonymous reviewers for their useful comments that helped improve the manuscript.

Received 5 November 2021; re-revised accepted 19 August 2022

doi: 10.18520/cs/v123/i7/933-938